European Society of Computational Methods in Sciences and Engineering (ESCMSE)

Journal of Numerical Analysis, Industrial and Applied Mathematics (JNAIAM)

vol. 2, no. 3-4, 2007, pp. 227-249
ISSN 1790–8140

New Variants of Deflation Techniques for Pressure Correction in Bubbly Flow Problems[1]

J.M. Tang[2] **C. Vuik**

Delft University of Technology,
J.M. Burgerscentrum,
Faculty of Electrical Engineering, Mathematics and Computer Science,
Delft Institute of Applied Mathematics,
Mekelweg 4, 2628 CD Delft,
The Netherlands.

Received 19 January, 2007; accepted in revised form 12 June, 2007

Abstract: For various applications, it is well-known that deflated ICCG is an efficient method to solve linear systems iteratively. This deflated ICCG can also be used to solve linear systems with a singular coefficient matrix arising from a discretization of the Poisson equation with Neumann boundary conditions and discontinuous coefficients. The use of sparse subdomain deflation vectors in this method appears to be very effective. In this paper, we explain this in more detail by applying a spectral analysis with perturbed eigenvectors.
Moreover, we introduce new variants of the deflation technique, that can deal with the pressure-correction equation for two-phase flow problems and in particular bubbly flow problems. The first variant is the deflation technique with the so-called levelset deflation vectors. In contrast to the standard subdomain deflation vectors, those vectors are related to the location of the bubbles in the domain. Another deflation variant uses the so-called levelset-subdomain deflation vectors and profits of the advantages of both subdomain and levelset deflation vectors. Numerical experiments show the good performance of these new deflation variants.

Keywords: deflation, conjugate gradient method, preconditioning, Poisson equation, symmetric positive semi-definite matrices, bubbly flow problems, level-set.

Mathematics Subject Classification: 65F10, 65F50, 65N22.

1 Introduction

Computation of two-phase flows, and in particular bubbly flows, is a very active research topic in computational fluid dynamics (CFD), see for instance [24, 28]. Bubbly flows are governed by the Navier-Stokes equations, that can be solved using an operator splitting method. In many of these

[1]Published electronically October 27, 2007
[2]Corresponding author. E-mail: J.M.Tang@tudelft.nl. Part of this research has been funded by the Dutch BSIK/BRICKS project.

popular operator splitting methods, a linear system for the pressure correction has to be solved for every time step, arising from a Poisson equation with discontinuous coefficients. This consumes the bulk of the computing time, although the coefficient matrix of this linear system is elliptic. The pressure correction equation is usually solved with the ICCG method, but this method shows slow convergence for complex bubbly flows, due to the occurrence of strongly varying coefficients, arising from the difference in density between bubbles and fluid. As an alternative for ICCG, we apply a deflated variant of ICCG, called DICCG, see, e.g., [8, 10, 15, 17, 19, 20, 21, 25, 34, 35]. The extra deflation technique removes the components of the eigenmodes that causes the slow convergence of ICCG.

For elliptic problems with large jumps in the coefficients (of which the pressure correction equation for bubbly flows is just one example), successful multigrid solvers and preconditioners can be found in, e.g., [2, 4, 36], whereas appropriate domain decomposition methods and preconditioners have been considered in, e.g., [7, 14, 27, 32]. However, here we restrict ourselves to DICCG-type methods, because it appears that these multigrid and domain decomposition methods show comparable results relative to DICCG, in our bubbly flow applications. Furthermore, the approach presented in this paper may be generalized to other preconditioners, which have comparable spectral properties.

Recently, DICCG applied to bubbly flows has been studied by the authors in [29, 30]. In [29], theoretical considerations of DICCG with subdomain deflation vectors are given, with respect to the singularity of the linear system. Moreover, 3D numerical experiments are described, comparing the number of iterations required for ICCG and DICCG. Furthermore, in [30], implementation issues of DICCG have been discussed related to efficiency. In addition, efficient methods to solve coarse linear systems within DICCG have been given, including a theoretical comparison of these methods. Finally, in [30], it is shown by numerical experiments that the proposed DICCG methods are very efficient. Compared with ICCG, DICCG decreased significantly the number of iterations and the computing time for which are required for efficiently solving the Poisson equation in applications to 2D and 3D bubbly flows.

However, in [29, 30], it has not been shown nor explained why the approach of DICCG with subdomain deflation vectors is successful. We have only conjectured that the smallest eigenvalues of the preconditioned coefficient matrix have been projected to zero, leading to fast convergence of DICCG. In this paper, it will be shown that this is indeed the case, by applying a spectral analysis with small perturbations in the eigenvectors associated with these smallest eigenvalues.

Furthermore, the subdomain deflation vectors are independent of the geometry of the bubbly flow. Hence, this DICCG approach can be used as a black-box method and can be easily and efficiently implemented in a computer code. But a drawback is that relevant physical information, which might improve DICCG significantly, is not exploited. Therefore, in this paper, we will give two new variants of DICCG, in which the deflation vectors are related to the bubble geometry.

The outline of this paper is as follows. Section 2 is devoted to the problem setting of the bubbly flow and properties of the resulting linear system. The deflation technique with general deflation vectors is introduced in Section 3. In Section 4, we investigate perturbations of the eigenvectors and their consequences for the deflation technique. Subsequently, new variants of the deflation method are introduced in Section 5. We describe some numerical experiments and a comparison is made between various deflation variants in Section 6. Finally, conclusions are drawn in Section 7.

2 Problem Setting

We consider a symmetric and positive semi-definite (SPSD) linear system

$$Ax = b, \quad A \in \mathbb{R}^{n \times n}, \tag{1}$$

where A is singular. The preconditioned variant (1) is given by

$$M^{-1}Ax = M^{-1}b, \quad M \in \mathbb{R}^{n\times n},$$

where M is a symmetric positive definite (SPD) preconditioner. In this paper, we restrict ourselves to the Incomplete Cholesky (IC) preconditioner [16], and the resulting preconditioned CG is called ICCG.

Assumption 1. *M is the IC preconditioner based on A.*

The linear system (1) is derived from a standard second-order finite-difference discretization of the 1D, 2D or 3D Poisson equation with variable coefficients and Neumann boundary conditions, that is

$$\begin{cases} -\nabla\cdot\left(\frac{1}{\rho(\mathbf{x})}\nabla p(\mathbf{x})\right) &= f(\mathbf{x}), \quad \mathbf{x}\in\Omega, \\ \frac{\partial}{\partial\mathbf{n}}p(\mathbf{x}) &= g(\mathbf{x}), \quad \mathbf{x}\in\partial\Omega, \end{cases} \tag{2}$$

where $p, \rho, \mathbf{x}$ and $\mathbf{n}$ denote the pressure, density, spatial coordinates and the unit normal vector to the boundary $\partial\Omega$, respectively. The problem is solved on a uniform Cartesian grid in a unit square domain Ω. Furthermore, we consider two-phase bubbly flows with for instance air (low density phase) and water (high density phase). In this case, ρ is piecewise constant with a contrast, ϵ, which is the ratio of the two densities, i.e.,

$$\rho = \begin{cases} \rho_0 = 1, & \mathbf{x}\in\Lambda_0, \\ \rho_1 = \epsilon & \mathbf{x}\in\Lambda_1, \end{cases}$$

where Λ_1 is the low density phase, namely bubbles in Ω, and Λ_0 is the high density phase, namely the fluid domain around these bubbles. Note that in the case of $\epsilon = 1$, we deal with the standard Poisson equation. For more details about the discretization and the above problem setting, see [23, 24].

The number of bubbles is denoted by $\omega \in \mathbb{N}$. Figure 1 shows the density field of a typical example with $\omega = 5$. Furthermore, $\Phi_i \subset \Omega$ denotes the domain corresponding to bubble i including its interface that may lie in Λ_0, for $i = 1, 2, \ldots, \omega$. Hence, we have

$$\Lambda_1 \subseteq \cup_{i=1}^{\omega}\Phi_i \quad \text{and} \quad \cap_{i=1}^{\omega}\Phi_i = \emptyset.$$

Since we use a uniform Cartesian grid with $n = n_x n_y$ cells in 2D, where n_x and n_y are the number of cells in the respective spatial direction. The discretized domain and the corresponding grid points are denoted by Ω_h and x_i, respectively. Moreover, Λ_{h_0}, Λ_{h_1} and Φ_{h_i} are the discretized variants of Λ_0, Λ_1 and Φ_i, respectively. For each $i = 1, \ldots, \omega$, we introduce the characteristic vector $\phi_i \in \mathbb{R}^n$ associated with bubble i, where each entry, $(\phi_i)_j$, is defined as follows:

$$(\phi_i)_j = \begin{cases} 1, & \text{if } x_j \in \Phi_{h_i}, \\ 0, & \text{elsewhere.} \end{cases}$$

Notice that the set of vectors $\{\phi_i\}_{i=1,\ldots,\omega}$ is linearly independent.

Define $\mathbf{1}_p$ and $\mathbf{0}_p$ as the all-one and all-zero vector with p elements, respectively. Given the fact that the solution of (2) is determined up to a constant, Assumption 2 is natural.

Assumption 2. *$A\mathbf{1}_n = \mathbf{0}_n$ and $b^T\mathbf{1}_n = 0$, and the algebraic multiplicity of the zero-eigenvalue of A is one.*

Eigenvalues of matrices will be sorted increasingly; that is, for each eigenvalue λ_i of $M^{-1}A$ we have $0 = \lambda_1 < \lambda_2 \leq \ldots \leq \lambda_n$. For $i > 2$, they appear to be of order 1, except for a few eigenvalues that are of order ϵ. The number of these $\mathcal{O}(\epsilon)-$eigenvalues depends on the number of bubbles, ω, see Proposition 1.

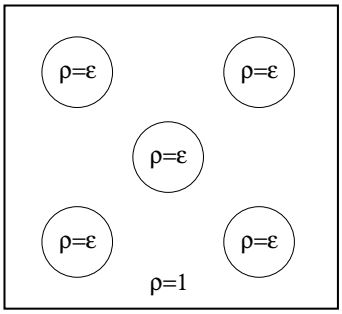

Figure 1: Density field ρ of a test problem with $\omega = 5$.

Proposition 1. *Let $1 < \omega < n$. Then, the eigenvalues λ_i of $M^{-1}A$ satisfy*

$$\lambda_i = \begin{cases} 0, & \text{for } i = 1; \\ \mathcal{O}(\epsilon), & \text{for } i = 2, \ldots, \omega; \\ \mathcal{O}(1), & \text{for } i = \omega + 1, \ldots, n. \end{cases}$$

Moreover, for $i = 2, \ldots, \omega$ each eigenvector v_i corresponding to λ_i is constant in Λ_1.

Hence, matrix $M^{-1}A$ has exactly $\omega - 1$ eigenvalues of $\mathcal{O}(\epsilon)$, if there are ω bubbles in Ω. Note that Proposition 1 still holds if bubbles meet the boundaries. Similar results have been proven in literature, see, e.g., [35, Thm. 2.2], where matrices are invertible and applications are given to steady porous media flows.

Obviously, if $\epsilon \ll 1$ and $\omega > 1$, then $M^{-1}A$ is ill-conditioned. Therefore, ICCG converges slowly. The method should be adapted such that it gets rid of these $\mathcal{O}(\epsilon)-$eigenvalues, resulting in a more efficient method. This can be realized by applying the deflation technique treated in the next section.

3 Deflation Technique

Extension of ICCG with the deflation technique leads to the deflated ICCG method (DICCG). In this section, we briefly describe this method.

Let the deflation subspace matrix $Z \in \mathbb{R}^{n \times k}$ with $k \ll n$ be given, consisting of k deflation vectors. The deflation matrix P is defined as follows:

$$P_Z := I - AZE^{-1}Z^T \in \mathbb{R}^{n \times n}, \quad E := Z^T AZ \in \mathbb{R}^{k \times k},$$

where E is assumed to be non-singular. We wish to solve the deflated system:

$$M^{-1}P_Z A\tilde{x} = M^{-1}P_Z b,$$

which is obviously singular. A solution x can be found from $\tilde{x}$ as follows ([19]):

$$x = ZE^{-1}Z^T b + P_Z^T \tilde{x}.$$

Let $\sigma(B) = \{\lambda_1, \lambda_2, \ldots, \lambda_n\}$ denote the spectrum of matrix B with eigenvalues λ_i and let $\widetilde{A} \in \mathbb{R}^{n \times n}$ be invertible. If Z has full rank, then Theorem 1 ensures that $M^{-1}P_Z\widetilde{A}$ has a more favorable spectrum than $M^{-1}\widetilde{A}$.

Theorem 1. *Let $\lambda_1 \leq \lambda_2 \leq \ldots \leq \lambda_n$ be the eigenvalues of $M^{-1}\widetilde{A}$, where $\widetilde{A} \in \mathbb{R}^{n\times n}$ is non-singular. Let $Z \in \mathbb{R}^{n\times k}$ be of full rank. Then*

$$\sigma(M^{-1}P_Z\widetilde{A}) = \{0,\ldots,0,\mu_{k+1},\ldots,\mu_n\},$$

with $\lambda_1 \leq \mu_i \leq \lambda_n$ for $i = k+1,\ldots,n$.

Proof. The result follows immediately from [33, Thm. 2.2]. □

It appears that a similar result holds for our singular matrix A:

- if $\mathbf{1}_n \in \mathrm{Col}(Z)$, then
$$\sigma(M^{-1}P_ZA) = \{0,\ldots,0,\mu_{k+1},\ldots,\mu_n\}, \tag{3}$$
with $\lambda_1 \leq \mu_i \leq \lambda_n$ for $i = k+1,\ldots,n$;
- if $\mathbf{1}_n \notin \mathrm{Col}(Z)$, then
$$\sigma(M^{-1}P_ZA) = \{0,\ldots,0,\mu_{k+2},\ldots,\mu_n\}, \tag{4}$$
with $\lambda_1 \leq \mu_i \leq \lambda_n$ for $i = k+2,\ldots,n$.

Note that the deflation subspace is larger for $\mathbf{1}_n \notin \mathrm{Col}(Z)$, compared to the case $\mathbf{1}_n \in \mathrm{Col}(Z)$. The above observations can be proven for specific choices of Z, see Theorem 5 in Section 5.2.

Of course, it depends on the deflation subspace matrix Z in which way the eigenvalues μ_i are distributed exactly, and therefore, the success of DICCG is related to the choice of Z. In the next section, we will discuss and analyze some appropriate choices for Z.

4 Analysis of Deflation with Perturbed Eigenvectors

In this section, we analyze the deflation technique, if we apply exact and perturbed eigenvectors corresponding to the eigenvalues of $\mathcal{O}(\epsilon)$.

4.1 Deflation with Exact Eigenvectors

According to Proposition 1, the most straightforward choice for the columns of Z is the set of eigenvectors corresponding to the $\mathcal{O}(\epsilon)-$eigenvalues, so that they are eliminated from the spectrum of $M^{-1}P_ZA$. This statement can be proven for $\widetilde{A}$, see Theorem 2.

Theorem 2 (Th. 2.5, [19])**.** *Let $\widetilde{A} \in \mathbb{R}^{n\times n}$ be non-singular. Let $M^{-1}\widetilde{A}$ have eigenvalues $\lambda_1 \leq \lambda_2 \leq \ldots \leq \lambda_n$ with corresponding eigenvectors v_i. If $V := [v_1\ v_2\ \cdots\ v_k]$, then*

$$\sigma(M^{-1}P_V\widetilde{A}) = \{0,\ldots,0,\lambda_{k+1},\ldots,\lambda_n\}.$$

Comparing Theorem 2 to Theorem 1, we see that $\mu_i = \lambda_i$, and therefore, each μ_i lies in $[\lambda_{k+1},\lambda_n]$ for $i = k+1,\ldots,n$. By observation, we note that, since $\mathbf{1}_n \in \mathrm{Col}(V)$, Theorem 2 also holds for our singular matrix A by replacing $\widetilde{A}$ by A. Hence, applying eigenvectors associated with $\mathcal{O}(\epsilon)-$eigenvalues as deflation vectors is a good strategy to improve the convergence of the iterative process. In this case, it is sufficient to take $k = \omega$, if one wants to eliminate all $\mathcal{O}(\epsilon)-$eigenvalues. Moreover, due to Assumption 2, v_1 is the constant eigenvector corresponding to the zero-eigenvalue. As a consequence, v_1 may be omitted in V, so that $k = \omega - 1$ deflation vectors would even be sufficient for the elimination of all $\mathcal{O}(\epsilon)-$eigenvalues.

Note that, although deflation with exact eigenvectors of $M^{-1}A$ leads to fast convergence, such a choice will in practice eventually lead to inefficiency. This is because these eigenvectors are usually dense and it is relatively expensive to compute and use them.

4.2 Deflation with Inexact Eigenvectors

Instead of using exact eigenvectors as deflation vectors, we could also use perturbed or approximated eigenvectors, such as Ritz vectors. Define $\bar{V} := [\bar{v}_1 \ \bar{v}_2 \ \cdots \ \bar{v}_k]$ where each $\bar{v}_i$ is an approximation of the exact eigenvector v_i of $M^{-1}A$, i.e.,

$$\bar{v}_i := v_i + \delta_i, \quad \delta_i \in \mathbb{R}^n, \quad i = 1, 2, \ldots, k, \quad \text{where } k \leq \omega. \tag{5}$$

Of course, it would be convenient that deflation with $\bar{V}$ has the same favorable features as deflation with V. If $k = \omega$, then the resulting spectrum of $M^{-1}P_{\bar{V}}A$ should not contain any eigenvalue of $\mathcal{O}(\epsilon)$ anymore. In this case, each δ_i has to be chosen in such a way that the eigenvalues of the resulting matrix $M^{-1}P_{\bar{V}}A$ satisfy

$$\mathcal{O}(\epsilon) \ll \bar{\lambda}_i \leq \lambda_n, \quad \text{for } i = k+1, \ldots, \omega, \tag{6}$$

where $\bar{\lambda}_i$ is an eigenvalue of $M^{-1}P_{\bar{V}}A$ and $\mathbf{1}_n \in \text{Col}\,(\bar{V})$ is assumed. However, as far as we know, in the literature no results are given concerning the way in which v_i can be perturbed, such that (6) is satisfied. In the remainder of this subsection, we will give some theoretical results and observations, resulting in heuristic rules for choosing δ_i. These are partly based on numerical experiments described in [31].

Define $\nu_i \in \mathbb{R}^n$ as the vector with the entries of $\bar{v}_i$, that correspond to the bubbles of phase Λ_1 including the interfaces, and let the other entries be zero, i.e., for each i, the entries of ν_i are defined by

$$(\nu_i)_j = \begin{cases} (\bar{v}_i)_j, & \text{if } \ x_j \in \Lambda_{h_1} \text{ or } x_j \in \partial\Lambda_{h_1}; \\ 0, & \text{otherwise,} \end{cases}$$

where $\partial\Lambda_{h_1}$ denotes the interfaces corresponding to Λ_{h_1}. Similar to ν_i, vector $\tilde{\mathbf{1}}_n \in \mathbb{R}^n$ is defined as follows:

$$(\tilde{\mathbf{1}}_n)_j = \begin{cases} 1, & \text{if } \ x_j \in \Lambda_{h_1} \text{ or } x_j \in \partial\Lambda_{h_1}; \\ 0, & \text{otherwise.} \end{cases}$$

Moreover, the perturbations satisfy Assumption 3.

Assumption 3. *Each perturbation $\delta_i \in \mathbb{R}^n$, with $i = 1, 2, \ldots, k$, is chosen such that*

1. *$||A\delta_i||_2 = \mathcal{O}(\epsilon)$ for each δ_i;*
2. *entries corresponding to at least one bubble in Λ_1 are nonzero in $\bar{v}_i$;*
3. *the set $\{\tilde{\mathbf{1}}_n, \nu_1, \ldots, \nu_k\}$ is linearly independent.*

The first condition of Assumption 3 means that the norm of the perturbation, after premultiplication with A, is small. The second condition says that it is not allowed to choose a perturbation δ_i in such a way that all elements of $\bar{v}_i$ corresponding to the bubbles are all zero. The final condition means that each δ_i should be chosen in such a way that all ν_i and $\tilde{\mathbf{1}}_n$ do not depend on each other.

Example 1. *In our bubbly flow applications, perturbations $\delta_i \in \mathbb{R}^n$ satisfy Assumption 3 in, for instance, the following two cases:*

- *choose arbitrary elements for the vector δ_i, corresponding to the high density phase Λ_0;*
- *choose arbitrary but identical elements of δ_i, corresponding to a complete bubble including its interface in the low density phase Λ_1, such that each δ_i corresponds to a different bubble.*

Next, define $V_\epsilon \in \mathbb{R}^{n\times k}$ with $k \leq \omega - 1$ as a matrix consisting of columns, which are eigenvectors of $M^{-1}A$ corresponding to $\mathcal{O}(\epsilon)-$eigenvalues. In addition, define $\bar{V}_\epsilon \in \mathbb{R}^{n\times k}$ as a perturbation of V_ϵ, so that each δ_i fulfills Assumption 3, i.e., each column of $\bar{V}_\epsilon$ is the sum of the corresponding column of V_ϵ and δ_i satisfying Assumption 3 (cf. Eq. (5)). Then it appears that Assumption 4 is always fulfilled in our experiments.

Assumption 4. *$P_{\bar{V}_\epsilon}A = P_{V_\epsilon}A + Q$ with $||Q||_2 = \mathcal{O}(\epsilon)$.*

In addition, define $\alpha \in \{0, 1, \ldots, \omega\}$ as the maximum number of characteristic vectors, ϕ_{h_i}, such that

$$\phi_{h_i} \subseteq \text{ span } \{\tilde{\mathbf{1}}_n, \nu_1, \ldots, \nu_k\}.$$

For instance, $\alpha = k$ means that the number of deflation vectors is equal to the number of vectors corresponding to separate bubbles, that can be constructed from the deflation subspace. Now, Theorem 3 follows easily.

Theorem 3. *Suppose that $\alpha = k$ and let Assumption 4 holds. Then, for $j = 1, \ldots, n$, we have*

$$|\lambda_j(P_{\bar{V}_\epsilon}A) - \lambda_j(P_{V_\epsilon}A)| \leq \gamma, \quad \gamma = \mathcal{O}(\epsilon). \tag{7}$$

Proof. Since $P_{\bar{V}_\epsilon}A = P_{V_\epsilon}A + Q$ with $||Q||_2 = \mathcal{O}(\epsilon)$, the theorem follows immediately from Corollary 8.1.6 of [11]. □

As a consequence of Theorem 3, perturbations δ_i that meet Assumption 3 do not significantly influence the spectrum of the deflated system $P_{V_\epsilon}A$. If, for instance, $P_{V_\epsilon}A$ does not contain $\mathcal{O}(\epsilon)-$eigenvalues, then neither does $P_{\bar{V}_\epsilon}A$.

Unfortunately, Theorem 3 can not be generalized to the preconditioned deflated systems, i.e., inequality (7) does not hold in general, if one substitutes $M^{-1}P_{\bar{V}}A$ and $M^{-1}P_V A$ for $P_{\bar{V}}A$ and $P_V A$, respectively. Counterexamples can be easily found using numerical experiments. It appears that only an adapted variant of Theorem 3 holds for the preconditioned case, see Proposition 2.

Proposition 2. *Let $k \in \{1, 2, \ldots, \omega - 1\}$ be given. Choose each $\delta_i \in \mathbb{R}^n$ such that Assumption 3 is fulfilled. Moreover, suppose that $\alpha = k$ and $\mathbf{1}_n \notin Col(V_{\bar{\epsilon}})$. Then,*

$$|\lambda_j(M^{-1}P_{\bar{V}_\epsilon}A) - \lambda_j(M^{-1}P_{V_\epsilon}A)| \leq \gamma, \quad \gamma = \mathcal{O}(\epsilon),$$

for all $j = 1, \ldots, \omega$.

According to Proposition 2, the $\mathcal{O}(\epsilon)-$eigenvalues of $M^{-1}P_{V_\epsilon}A$ are not significantly influenced by these perturbations, if each perturbation δ_i is chosen such that Assumption 3 is satisfied. However, Proposition 2 does not say anything about the other eigenvalues of $M^{-1}P_{V_\epsilon}A$. Fortunately, it can be observed that the number of $\mathcal{O}(\epsilon)-$eigenvalues is equal for $M^{-1}P_{V_\epsilon}A$ and $M^{-1}P_{\bar{V}_\epsilon}A$, if $\alpha = k$. Moreover, a similar result follows for $\alpha < k$. These results are stated in Conjecture 1.

Conjecture 1. *Let $k \in \{1, 2, \ldots, \omega - 1\}$ be given and suppose $\alpha = k$. Choose each $\delta_i \in \mathbb{R}^n$ so that Assumption 3 is fulfilled. Then, the number of $\mathcal{O}(\epsilon)-$eigenvalues of $M^{-1}P_{\bar{V}_\epsilon}A$ is equal to*

$$\begin{cases} \omega - \alpha - 1, & \text{if } \alpha < \omega - 1; \\ 0, & \text{if } \alpha \geq \omega - 1. \end{cases}$$

Moreover, if $\alpha \geq k$, then the number of $\mathcal{O}(\epsilon)-$eigenvalues of both $M^{-1}P_{\bar{V}_\epsilon}A$ and $M^{-1}P_{V_\epsilon}A$ is the same.

As a special case of Conjecture 1, we have that both $M^{-1}P_{\bar{V}_\epsilon}A$ and $M^{-1}P_{V_\epsilon}A$ do not contain any $\mathcal{O}(\epsilon)$-eigenvalue, if $k = \omega - 1$ and each $\tilde{\delta}_i$ has nonzero entries associated with at least one bubble. Example 2 shows another application of the conjecture.

Example 2. *Consider a 2D bubbly flow problem with $\omega = 5$, see Figure 2. In this case, the spectrum of $M^{-1}A$ contains four $\mathcal{O}(\epsilon)-$eigenvalues. The corresponding eigenvectors are taken as the deflation vectors. As seen in Figure 2, two situations are considered, where Ω has been divided into four (deflation) subdomains Ω_i, each corresponding to one perturbation vector δ_i, whose entries are constant in this subdomain and zero elsewhere. In the case given in Figure 2(a), none of the perturbations satisfy Assumption 3. Therefore, all four $\mathcal{O}(\epsilon)-$eigenvalues of $M^{-1}A$ remain in the spectrum of $M^{-1}P_{\bar{V}_\epsilon}A$. However, in the case of Figure 2(b), all perturbations meet Assumption 3, but obviously $\alpha = 3$. According to Conjecture 1, the spectrum of $M^{-1}P_{\bar{V}_\epsilon}A$ consists of exactly one $\mathcal{O}(\epsilon)$-eigenvalue, which can be easily confirmed by numerical experiments.*

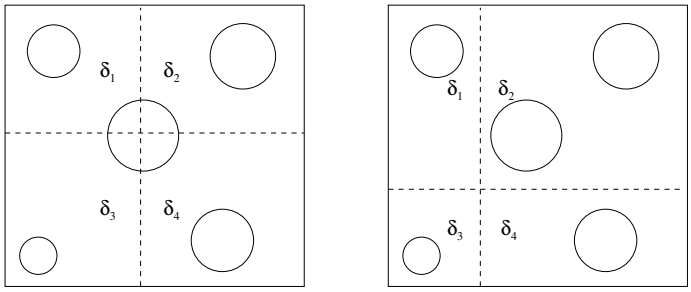

(a) Wrong choice of subdomains, since the middle bubble is not captured by one subdomain.

(b) Good choice of subdomains, since each bubble is in the interior of a subdomain.

Figure 2: A 2D example of a bubbly flow problem with $\omega = 5$ and two different situations for the perturbations δ_i.

Moreover, from Conjecture 1, we obtain the unexpected result that a good strategy for choosing an appropriate deflation vector $\bar{v}_i = v_i + \delta_i$ is related to $A\delta_i$, rather than to $M^{-1}A\delta_i$.

Finally, we refer to [26] for related results concerning the choice of deflation vectors. In that paper, two-level overlapping domain decomposition preconditioners with coarse spaces have been studied, by smoothed aggregation in iterative solvers for finite element discretizations of elliptic problems. Furthermore, similar observations as made in this section have been proven using functional analysis. It is a topic of current research to extend the theory given in [26] to the deflation strategies here.

5 Variants of Deflation

In the previous section, we have seen that exact eigenvectors are not required to eliminate the smallest eigenvalues from the spectrum of $M^{-1}P_Z A$. Conjecture 1 can serve as a guideline for approximating eigenvectors corresponding to $\mathcal{O}(\epsilon)-$eigenvalues. This leads to strategies for choosing effective deflation vectors. In the next subsections, the resulting deflation variants will be described.

5.1 Levelset Deflation

By combining the results obtained in Example 1 and Conjecture 1, it can be concluded that eigenvectors v_i associated with the $\mathcal{O}(\epsilon)-$eigenvalues are still well-approximated, if

- all entries of v_i, corresponding to a bubble of Λ_1 including its interface $\partial\Lambda_1$, are scaled by a constant. Therefore, for convenience, the value 1 can be chosen for the associated entries of

the perturbed eigenvector $\bar{v}_i$, since we know from Assumption 1 that all elements in a bubble are constant;

- the entries of v_i corresponding to the high density phase Λ_0 can be perturbed arbitrarily. To obtain sparse perturbed eigenvectors $\bar{v}_i$, it is convenient to perturb these elements of v_i, such that they become zero. In other words, $(\bar{v}_i)_j = 0$, if $x_j \in \Lambda_{h_0}$ and $x_j \notin \partial\Lambda_{h_1}$.

Hence, each v_i can be approximated well by a sparse $\bar{v}_i$ such that only the entries corresponding to bubbles are nonzero. From Conjecture 1, we also find that if $\alpha \geq \omega - 1$ then all $\mathcal{O}(\epsilon)-$eigenvalues of $M^{-1}A$ can be eliminated by choosing $k = \omega - 1$. The requirement $\alpha \geq \omega - 1$ is automatically fulfilled when we associate each $\bar{v}_i$ to one unique bubble, so that only the entries corresponding to a single bubble are nonzero. Note that one bubble of Ω is excluded, since $k = \omega - 1$. The resulting deflation subspace matrix with vectors $\bar{v}_i$ will be denoted by $W_{\text{L}} \in \mathbb{R}^{n\times k}$, and the resulting deflation method is called L-DICCG$-k$, where k is always chosen to be $\omega - 1$. We define $\widetilde{W}_{\text{L}} \in \mathbb{R}^{n\times\omega}$ as $W_{\text{L}} \in \mathbb{R}^{n\times(\omega-1)}$, extended with a column associated with the excluded bubble. Later on, $\widetilde{W}_{\text{L}}$ will be used to define the levelset-subdomain deflation variant.

Note that, if some bubbles in Ω are very close to each other, then some grid points x_i might belong to the same nonzero elements of several columns of W_{L}. In this case, row sums of W_{L} can be larger than one, resulting in non-disjunct columns. This is, however, not a drawback of the method. On the contrary, if one avoids the disjunction of the vectors, by choosing zero instead of one at some entries associated with the bubble interface, then the corresponding eigenvectors appear to be approximated badly. This results in slower convergence of the iterative process, see also Section 6.5.2.

If the density field ρ is known explicitly, then L-DICCG$-k$ can be simply applied by locating the bubbles in Λ_1, and choosing one for the corresponding entries of the columns of W_{L}. However, in many applications, ρ is only given implicitly. For example, the levelset approach [18, 22] has been adopted to describe ρ implicitly in our applications, see e.g. [23, 24, 30]. In this approach, the interfaces of the bubbles are defined by the zero level-set of a marker function Ψ: $\Psi = 0$ at the interface, $\Psi > 0$ inside the high density phase Λ_1 and $\Psi < 0$ elsewhere. The interface is implicitly advected, by advecting Ψ as if it were a material property:

$$\frac{\partial\Psi}{\partial t} + u \cdot \nabla\Psi = 0,$$

where u is the velocity vector in Ω. Therefore, ρ can be determined at each time step, without having the exact coordinates of each bubble. For choosing deflation vectors, an extra procedure for determining the bubbles from Ψ should be carried out. For example, Algorithm 1 gives the pseudo-code, that can be used for 2D problems on an equidistant grid [3]. In this algorithm, $\hat{x}_i$ denotes an adjacent grid point corresponding to x_i.

In Algorithm 1, three loops are needed to distinguish the bubbles from the rest of the domain and to include their adjacent grid points, requiring $\mathcal{O}(n)$ flops. Note further that, in the case of deciding whether a grid point is in a bubble, we simply look at the sign of the corresponding element of Ψ. If the value is positive, the grid point is in the interior of the bubble, if it is negative, then it is outside the bubble, and otherwise, it is on the interface. In this way, it is straightforward to determine the bubbles from the levelset function, and to obtain a code where each deflation vector corresponds to exactly one bubble. The algorithm is further explained in Example 3.

Example 3. *A 2D bubbly flow problem with $\omega = 3$ bubbles is considered, see Figure 3. In each of the subplots, one can see the intermediate and final results of applying Algorithm 1 to determine each bubble.*

[3] If the computations would be applied to an unstructured grid, similar algorithms as Algorithm 1 can be used, where for instance reordering strategies like Cuthill McKee's algorithm [3] might be exploited.

Algorithm 1 Determination of bubbles from the levelset function in 2D

set $j = 1$ and $f = \mathbf{0}_n$;
for x_1 to x_n (from left to right and from bottom to top) **do**
  if $x_i \in \Lambda_{h_1}$ **then**
    if left and/or bottom $\hat{x}_i \notin \Lambda_{h_1}$ **then**
      $f_i = j$;
      $j = j + 1$;
    else
      $f_i = \min_{\hat{x}_i} f$;
    end if
  end if
end for
for x_n to x_1(from right to the left and from top to bottom) **do**
  if $x_i \in \Lambda_{h_1}$ **then**
    if right and/or top $\hat{x}_i \notin \Lambda_{h_1}$ **then**
      $f_i = j$;
      $j = j + 1$;
    else
      $f_i = \min_{\hat{x}_i} f$;
    end if
  end if
end for
Renumber all $f_i \neq 0$;
for x_1 to x_n **do**
  if $x_i \in \Lambda_{h_1}$ and $\hat{x}_i \notin \Lambda_{h_1}$ **then**
    $f_{\hat{x}_i} = f_i$;
  end if
end for

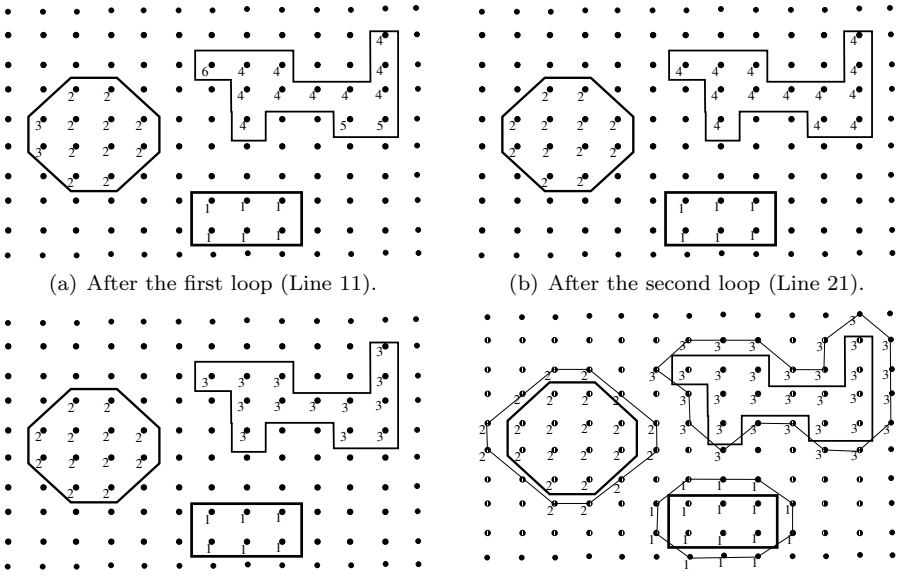

(a) After the first loop (Line 11). (b) After the second loop (Line 21).

(c) After renumbering (Line 22). (d) After the algorithm (Line 27).

Figure 3: A 2D bubbly flow problem with $\omega = 3$, to show the application of Algorithm 1. The numbers given in the plots are the corresponding values of vector f.

5.2 Subdomain Deflation

In bubbly flow problems, where Ω contains many bubbles, or where the density field ρ is unknown or too complex, it is more convenient to apply the deflation technique with the original subdomain deflation vectors instead of levelset deflation vectors. These subdomain vectors are constructed without any knowledge of ρ. For example, in [29, 30], we used squares and cubes as subdomains in 2D and 3D applications, respectively. We denote the deflation method with subdomain vectors as S-DICCG$-k$, where k is the number of subdomains minus one. Moreover, $W_{\text{S}} \in \mathbb{R}^{n\times k}$ denotes the corresponding deflation subspace matrix, which will be defined in a more mathematical way below.

Let Ω be divided into open (equal) subdomains $\Omega_i,\ i = 1, 2, \ldots, m$, such that $\overline{\Omega} = \cup_{i=1}^{m} \overline{\Omega}_i$ and $\Omega_i \cap \Omega_j = \emptyset$ for all $i \neq j$. The discretized subdomains are denoted by Ω_{h_i}. For each Ω_{h_i}, we introduce a deflation vector z_i as follows:

$$(z_i)_j := \begin{cases} 0, & x_j \in \Omega_h \setminus \overline{\Omega}_{h_i}; \\ 1, & x_j \in \Omega_{h_i}. \end{cases}$$

Then, W_{S} is defined by

$$W_{\text{S}} := [z_1\ z_2\ \cdots\ z_{m-1}],$$

so that $k = m - 1$. Hence, W_{S} consists of disjunct and orthogonal piecewise-constant vectors, which is generally not the case for W_{L}. Moreover, note that W_{S} is usually less sparse and consists of more vectors than W_{L}, and the amount of work is $\mathcal{O}(n)$ for the construction of both W_{S} and W_{L}.

We could also extend W_{S} with an extra column z_m, which results in

$$\widetilde{W}_{\text{S}} := [z_1\ z_2\ \cdots\ z_m].$$

The deflation subspace matrix W_{s} will be used later on. Note that each subdomain corresponds to one deflation vector, and we have the identity

$$\widetilde{W}_{\mathrm{s}}\mathbf{1}_m = \mathbf{1}_n. \tag{8}$$

It can be shown that W_{s} and $\widetilde{W}_{\mathrm{s}}$ lead to the same deflation matrix, since $\mathbf{1}_n \in \mathrm{Col}(\widetilde{W}_{\mathrm{s}})$. This is stated in Theorem 4.

Theorem 4 (Th. 4.6, [30]). *The following identity holds:*

$$M^{-1}P_{W_S}A = M^{-1}P_{\widetilde{W}_S}A.$$

Note that Eq. (8) is a useful property with respect to the implementation and some proofs of theoretical results. But recall that this may give rise to difficulties for approximating the eigenvalues associated with the bubbles, especially if bubbles are very close to each other. To approximate the corresponding eigenvectors appropriately, some row sums of W_{s} should be larger than one.

Because of Conjecture 1, we find that S-DICCG$-k$ can only be efficient, if each subdomain Ω_j contains a part of at most one bubble. Otherwise, one or more $\mathcal{O}(\epsilon)-$eigenvalues will remain in the spectrum of $M^{-1}P_{W_{\mathrm{S}}}A$. Hence, to ensure the efficiency of the method, the number of subdomains, k, should be taken very large, compared with the number of bubbles.

We find that the subdomain deflation vectors also approximate other eigenvectors corresponding to small eigenvalues of $\mathcal{O}(1)$, since they appear to vanish from the spectrum of $M^{-1}P_{W_{\mathrm{S}}}A$, for sufficiently large k. In Section 6, we will illustrate this with numerical experiments, but we will already state that in Proposition 3.

Proposition 3. *For sufficiently large k, Col(W_s) consists of vectors that are good approximations of the eigenvectors corresponding to the smallest $\mathcal{O}(1)$-eigenvalues.*

Hence, S-DICCG$-k$ is able to eliminate both $\mathcal{O}(\epsilon)-$ and $\mathcal{O}(1)-$eigenvalues from $M^{-1}A$. This means that, although S-DICCG$-k$ is usually more expensive per iteration than L-DICCG$-k$, the total computational cost can be much less due to faster convergence.

Finally, we end with Theorem 5, that extends Theorem 1 to singular coefficient matrices for specific choices of Z.

Theorem 5. *Let $0 = \lambda_1 < \lambda_2 \leq \ldots \leq \lambda_n$ be the eigenvalues of $M^{-1}A$. Then,*

$$\sigma(M^{-1}P_{W_S}A) = \{0, \ldots, 0, \mu_{k+1}, \ldots, \mu_n\}, \tag{9}$$

with $\lambda_1 \leq \mu_i \leq \lambda_n$ for all $i = k+1, \ldots, n$.

Proof. By Theorem 2 of [29], we have that

$$M^{-1}P_{W_{\mathrm{S}}}\widetilde{A} = M^{-1}\widehat{P}_{\widetilde{W}_{\mathrm{S}}}\widehat{A},$$

for some invertible matrix $\widehat{A}$ and corresponding deflation matrix $\widehat{P}_{\widetilde{W}_{\mathrm{S}}}$. Then, (9) follows immediately from Theorem 1 and Theorem 4. □

5.3 Levelset Subdomain Deflation

For density fields ρ with a complex geometry, S-DICCG$-k$ with large k may have difficulties to get rid of all $\mathcal{O}(\epsilon)-$eigenvalues, although the smallest $\mathcal{O}(1)-$eigenvalues can be eliminated. On the other hand, L-DICCG$-k$ with $k = \omega - 1$ easily deals with these $\mathcal{O}(\epsilon)-$eigenvalues, while the $\mathcal{O}(1)-$eigenvalues are untouched. Therefore, it can be beneficial to combine both variants.

This new deflation variant is called LS-DICCG$-k$, while $W_{\text{LS}} \in \mathbb{R}^{n\times k}$ denotes its corresponding deflation subspace matrix. The exact form of W_{LS} will be defined below.

First, we define some simple operations on matrices. The operation $\cup Y \in \mathbb{R}^{r\times 1}$, acting on $Y = [y_{i,j}] \in \mathbb{R}^{r\times s}$, means that a vector is created whose entries are the maximum elements of each row of Y, i.e., we have $(\cup Y)_i = \max_j y_{i,j}$ for each i, requiring $\mathcal{O}(r)$ flops. Moreover, for $Y_1 \in \mathbb{R}^{r\times s_1}$ and $Y_2 \in \mathbb{R}^{r\times s_2}$, the operation $Y_1 \cap Y_2 \in \mathbb{R}^{r\times s_3}$ means that a new matrix (or vector) is created, whose columns are equal to all possible componentwise multiplications between the columns of Y_1 and Y_2, that are non-zero. Note that $s_3 \leq s_1 s_2$ and the amount of work for this operation is at most $\mathcal{O}(r s_1 s_2)$.

Then, we define

$$\widetilde{W}_{\text{LS}} := [W_1, W_2], \tag{10}$$

with

$$W_1 := \widetilde{W}_{\text{S}} \cap (\mathbf{1}_n - \cup\widetilde{W}_{\text{L}}), \quad W_2 := \widetilde{W}_{\text{L}} \cap \widetilde{W}_{\text{S}}. \tag{11}$$

Hence, W_1 consists of all subdomain vectors of W_{S}, where the entries corresponding to Λ_1 are zero. Moreover, W_2 consists of columns, whose entries correspond to the bubbles, divided by the subdomains of $\widetilde{W}_{\text{S}}$.

The levelset subdomain deflation subspace matrix W_{LS} is equal to

- $\widetilde{W}_{\text{LS}}$, if $\mathbf{1}_n \notin \text{Col}\ (\widetilde{W}_{\text{LS}})$;
- $\widetilde{W}_{\text{LS}}$ without its last column, if $\mathbf{1}_n \in \text{Col}\ (\widetilde{W}_{\text{LS}})$.

Note again that that both W_{LS} and $\widetilde{W}_{\text{LS}}$ lead to the same deflation matrix. Example 4 is used to illustrate the construction of W_{LS}.

Example 4. *Let*

$$\widetilde{W}_S = \begin{bmatrix} 1 & 1 & 1 & 1 & 0 & 0 & 0 & 0 \\ 0 & 0 & 0 & 0 & 1 & 1 & 1 & 1 \end{bmatrix}^T, \quad \widetilde{W}_L = \begin{bmatrix} 0 & 1 & 1 & 0 & 0 & 0 & 0 & 0 \\ 0 & 0 & 0 & 0 & 0 & 1 & 1 & 0 \end{bmatrix}^T$$

be the deflation subspace matrices, corresponding to S-DICCG-2 and L-DICCG-2, respectively. Then, this yields

$$\cup\widetilde{W}_L = \begin{bmatrix} 0 & 1 & 1 & 0 & 0 & 1 & 1 & 0 \end{bmatrix}^T, \quad \boldsymbol{1}_n - \cup\widetilde{W}_L = \begin{bmatrix} 1 & 0 & 0 & 1 & 1 & 0 & 0 & 1 \end{bmatrix}^T,$$

resulting in

$$W_1 = \widetilde{W}_S \cap (\boldsymbol{1}_n - \cup\widetilde{W}_L) = \begin{bmatrix} 1 & 0 & 0 & 1 & 0 & 0 & 0 & 0 \\ 0 & 0 & 0 & 0 & 1 & 0 & 0 & 1 \end{bmatrix}^T,$$

and

$$W_2 = \widetilde{W}_L \cap \widetilde{W}_S = \begin{bmatrix} 0 & 1 & 1 & 0 & 0 & 0 & 0 & 0 \\ 0 & 0 & 0 & 0 & 0 & 1 & 1 & 0 \end{bmatrix}^T.$$

This implies

$$\widetilde{W}_{LS} = [W_1, W_2] = \begin{bmatrix} 1 & 0 & 0 & 1 & 0 & 0 & 0 & 0 \\ 0 & 0 & 0 & 0 & 1 & 0 & 0 & 1 \\ 0 & 1 & 1 & 0 & 0 & 0 & 0 & 0 \\ 0 & 0 & 0 & 0 & 0 & 1 & 1 & 0 \end{bmatrix}^T.$$

Finally, since $\boldsymbol{1}_n \in$ Col $(\widetilde{W}_{LS})$, the levelset-subdomain deflation subspace matrix W_{LS} is equal to

$$W_{LS} = \begin{bmatrix} 1 & 0 & 0 & 1 & 0 & 0 & 0 & 0 \\ 0 & 0 & 0 & 0 & 1 & 0 & 0 & 1 \\ 0 & 1 & 1 & 0 & 0 & 0 & 0 & 0 \end{bmatrix}^T.$$

Note that

$$\begin{cases} \text{Col}\,(\widetilde{W}_{\text{S}}) & \subseteq & \text{Col}\,(\widetilde{W}_{\text{LS}}); \\ \text{Col}\,(\widetilde{W}_{\text{L}}) & \subseteq & \text{Col}\,(\widetilde{W}_{\text{LS}}), \end{cases}$$

which means that the deflation subspace of LS-DICCG$-k$ consists of the deflation subspaces of both L-DICCG$-k$ and S-DICCG$-k$. In addition, observe that if W_{L} consists of non-disjunct deflation vectors, then $\widetilde{W}_{\text{LS}}\mathbf{1}_k \neq \mathbf{1}_n$.

Note that the construction of W_{LS} requires at most $\mathcal{O}(nm\omega)$ flops, where m is the number of subdomains chosen in the subdomain deflation variant. In addition, compared with L-DICCG$-k$ and S-DICCG$-k$, LS-DICCG$-k$ requires more deflation vectors, so an iteration of this hybrid method is more expensive due to the more sophisticated coarse solves. However, since the spectrum of $M^{-1}P_{W_{\text{LS}}}A$ is more favorable, convergence can be much faster, resulting in a lower total computational cost of LS-DICCG$-k$.

Furthermore, we remark that another variant of LS-DICCG$-k$ can be used, where $\widetilde{W}_{\text{LS}}$ is defined by $\widetilde{W}_{\text{LS}} := [\widetilde{W}_L, \widetilde{W}_S]$ with corresponding W_{LS}. This alternative saves some setup time and a fewer number of deflation vectors is required, compared with the original LS-DICCG$-k$. The drawback is that row sums larger than one are inevitable. This is left for further research.

We end this section with Example 5, that illustrates the deflation variants proposed in this section.

Example 5. *Consider a 2D bubbly flow problem with $\omega = 5$. The associated deflation vectors in L-DICCG-4, S-DICCG-3 and the resulting LS-DICCG-11 are depicted graphically in Figure 4.*

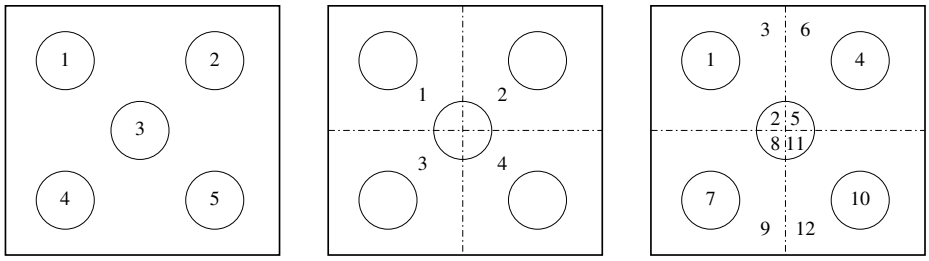

(a) L-DICCG-4 ($k = \omega - 1$). (b) S-DICCG-3 ($m = 4$). (c) LS-DICCG-11 ($k < m\omega$).

Figure 4: A 2D bubbly flow problem with $\omega = 5$, illustrating the levelset, subdomain and levelset subdomain deflation technique.

6 Numerical Experiments

In this section, we perform some 2D numerical experiments to test the three deflation variants, L-DICCG$-k$, S-DICCG$-k$ and LS-DICCG$-k$. These variants will be compared with ICCG. The computations are performed on a Pentium 4 (2.80 GHz) computer with a memory capacity of 1GB using MATLAB.

First, we consider briefly the test problem without bubbles, that is the Poisson problem with a contrast $\epsilon = 1$. Next, we treat the test problem with bubbles, where we vary grid sizes n, contrast ϵ and the number of bubbles ω. The employed geometry of the density field ρ with $\omega = 5$ can be found in Figures 1 and 4.

For the iterative solvers, a random starting vector x_0 will be used. The following termination criterion is applied:

$$\frac{||M^{-1}P_Z(b - A\tilde{x}_k)||_2}{||M^{-1}(b - Ax_0)||_2} < 10^{-7},$$

for each variant of DICCG with corresponding deflation matrix P_Z. This is equivalent to the standard termination criterion in ICCG, that is

$$\frac{||M^{-1}(b - Ax_k)||_2}{||M^{-1}(b - Ax_0)||_2} < 10^{-7}.$$

6.1 Poisson Problem with $\epsilon = 1$ and $n = 16^2$

Since there are no bubbles in the domain, only S-DICCG$-k$ can be applied to the Poisson problem with $\epsilon = 1$. The results are presented in Table 1.

Method	# It.
ICCG	23
S-DICCG-3	22
S-DICCG-15	15
S-DICCG-63	10

Table 1: Convergence results of the Poisson problem with $\epsilon = 1$ and $n = 16^2$. '# It' means the number of required iterations for convergence.

From Table 1, it can be noticed that S-DICCG$-k$ reduces the number of iterations, compared with ICCG. The corresponding eigenvalues of $M^{-1}A$ and $M^{-1}P_{W_S}A$ can be found in Figure 5.

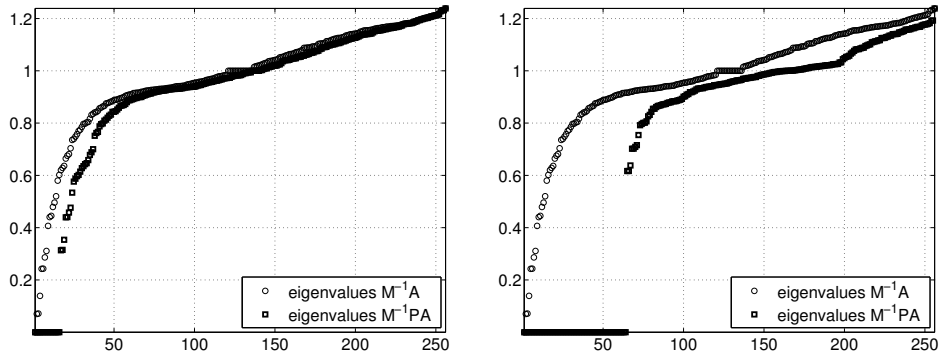

(a) S-DICCG-15 (15 iterations). (b) S-DICCG-63 (10 iterations).

Figure 5: Eigenvalues of $M^{-1}A$ and $M^{-1}P_{W_S}A$ for S-DICCG$-k$, applied to the Poisson problem with $\epsilon = 1$ and $n = 16^2$.

From both subplots of Figure 5, we observe that small $\mathcal{O}(1)-$eigenvalues of $M^{-1}A$ have been eliminated from the spectrum of $M^{-1}P_{W_S}A$ (see also Proposition 3), whereas the large eigenvalues remain in the spectrum. Increasing the number of deflation vectors results in the elimination of more small eigenvalues. This can be explained by the fact that the corresponding eigenvectors are relatively smooth, so that they can be well-approximated by the subdomain deflation vectors. Other eigenvectors corresponding to larger eigenvalues of $M^{-1}A$ do not have a smooth behavior,

and therefore, these are more difficult to approximate by using the subdomain deflation vectors, see also [31, Sect. 10.1].

6.2 Poisson Problem with $\omega = 5$, $\epsilon = 10^{-6}$ and Varying Grid Sizes

In this subsection, we will perform numerical experiments for the Poisson problem with $\omega = 5$, $\epsilon = 10^{-6}$ and varying grid sizes. The convergence results, including the computational cost, can be found in Table 2. The cost is given in terms of the computational time that is required for the whole iteration process. [4]

		$n = 16^2$		$n = 32^2$		$n = 64^2$	
Deflation Method	k	# It.	CPU	# It.	CPU	# It.	CPU
ICCG	–	39	0.04	82	0.53	159	10.92
S-DICCG$-k$	3	37	0.12	80	0.67	194	14.01
	15	36	0.07	97	0.80	193	13.82
	63	19	0.11	16	0.20	26	2.14
L-DICCG$-k$	4	17	0.09	37	0.37	75	6.17
LS-DICCG$-k$	11	14	0.07	30	0.29	54	4.08
	35	10	0.08	21	0.32	40	3.05
	83	–	–	15	0.20	25	2.05

Table 2: Convergence results for the Poisson problem with $\omega = 5$, $\epsilon = 10^{-6}$ and varying grid sizes. '# It' means the number of required iterations, and 'CPU' means the corresponding computational time in seconds.

For all grid sizes, it can be observed that S-DICCG-63 is very efficient, compared with ICCG. This is in contrast to S-DICCG-3 and S-DICCG-15, whose performance is comparable to ICCG. The explanation is that Assumption 3 is fulfilled only for $k = 63$, and according to Conjecture 1, the spectrum associated with S-DICCG-63 does not contain $\mathcal{O}(\epsilon)-$eigenvalues, see also Section 6.5. For the other two cases, S-DICCG-3 and S-DICCG-15, some deflation subdomains consist of parts of several bubbles, and therefore, the corresponding deflation vectors do not satisfy Assumption 3. Hence, the number of $\mathcal{O}(\epsilon)-$eigenvalues will not be reduced by the subdomain deflation vectors. Furthermore, note that in the case of $n = 64^2$, ICCG requires significantly fewer iterations than S-DICCG-3 and S-DICCG-15. This is caused by the fact that the corresponding residuals show erratic behavior with relatively large bumps, so that a small rounding error during the iteration process can lead to significant differences in convergence, see [31, Sect. 10.3] for more details.

Moreover, we see from Table 2 that L-DICCG$-k$ reduces significantly the number of iterations. It is an efficient method, since it requires only four deflation vectors.

We find that LS-DICCG$-k$ performs very well in all cases, but S-DICCG$-k$ and LS-DICCG$-k$ become comparable for sufficiently large k. Important to note is that, if there are some limitations with respect to the number of deflation vectors due to memory capacity, then LS-DICCG$-k$ converges faster than S-DICCG$-k$. Suppose that only $k < 50$ deflation vectors can be kept in memory, than the fastest method is LS-DICCG-35.

Some related spectral analysis will be given in Section 6.5.

[4] This is including the computation of AZ and E, but excluding the construction of Z since it can not be done efficiently in MATLAB. However, the comparison is still fair, since the computational cost to construct Z is negligible by considering the flop counts given in Section 5.

6.3 Poisson Problem with $\omega = 5$, $n = 64^2$ and Varying Contrasts

In this subsection, we fix $\omega = 5$ and $n = 64^2$, whereas the contrast, ϵ, is varied in the numerical experiments. The results are given in Table 3.

		$\epsilon = 10^{-3}$		$\epsilon = 10^{-6}$	
Deflation Method	k	# It.	CPU	# It.	CPU
ICCG	–	118	8.12	159	10.92
S-DICCG$-k$	3	134	9.79	194	14.01
	15	131	9.60	193	13.82
	63	26	2.31	26	2.14
L-DICCG$-k$	4	74	5.98	75	6.17
LS-DICCG$-k$	11	54	4.05	54	4.08
	35	40	3.08	40	3.05
	83	25	2.46	25	2.41

Table 3: Convergence results for the Poisson problem with $\omega = 5$, $n = 64^2$ and varying contrast ϵ.

From Table 3, we see that ICCG requires more iterations and CPU time for smaller ϵ, due to the presence of $\mathcal{O}(\epsilon)-$eigenvalues in the corresponding spectrum. This observation does not hold for L-DICCG$-k$ and LS-DICCG$-k$, which is a favorable feature of these methods, and it confirms the theory given in the previous section. For sufficiently large k, it can be noticed that S-DICCG$-k$ is also insensitive to ϵ.

Again, it can be observed that S-DICCG-3 and S-DICCG-15 converge more slowly than ICCG, whereas S-DICCG-63 is faster.

6.4 Poisson Problem with $\epsilon = 10^{-6}$, $n = 64^2$ and Varying Number of Bubbles

We consider the Poisson problem with $\epsilon = 10^{-6}$, $n = 64^2$ and a varying number of bubbles ω. The results can be found in Table 4.

One observes that ICCG needs more iterations, for larger ω. This can be explained by Proposition 1, which states that an increase of ω leads to more $\mathcal{O}(\epsilon)-$eigenvalues. For L-DICCG$-k$, LS-DICCG$-k$, and S-DICCG$-k$ with sufficiently large k, we see that their performance depends less on ω, which is a favorable feature of these deflation variants.

Notice that L-DICCG-0 is undefined, so this method can not be applied for $\omega = 1$. Furthermore, L-DICCG$-k$ converges in fewer iterations for increasing $\omega > 1$. Finally, S-DICCG$-k$ converges again more slowly than ICCG, for $k \leq 15$.

All variants of the deflation method (except for S-DICCG$-k$ with relatively small k) hardly depend on ω, in contrast to ICCG. This means that for problems with more bubbles, the deflation method can even be more efficient.

6.5 Analysis of Small Eigenvalues for all Deflation Variants

In this subsection, we give some eigenvalue plots corresponding to the deflation variants. These are based on the numerical experiment described in Section 6.2.

6.5.1 Subdomain Deflation

In Section 6.2, we have seen that S-DICCG-15 does not give any improvement of the convergence, whereas S-DICCG-63 is very efficient, compared with ICCG. This can be understood by consid-

	$\omega = 1$			$\omega = 2$			$\omega = 5$		
Deflation Method	k	# It.	CPU	k	# It.	CPU	k	# It.	CPU
ICCG	–	89	6.13	–	104	7.20	–	159	10.92
S-DICCG$-k$	3	96	7.39	3	69	5.13	3	194	14.01
	15	52	3.97	15	64	4.79	15	193	13.82
	63	26	2.14	63	27	2.16	63	26	2.14
L-DICCG$-k$	0	–	–	1	79	5.79	4	75	6.17
LS-DICCG$-k$	7	67	5.30	6	65	5.11	11	54	4.08
	19	41	3.14	24	42	3.22	35	40	3.05
	67	26	2.50	72	26	2.11	83	25	2.05

Table 4: Convergence results for the Poisson problem with $\epsilon = 10^{-6}$, $n = 64^2$ and varying number of bubbles.

ering their spectral plots, see Figure 6. Because we concentrate on small eigenvalues, only the 80 smallest eigenvalues of the corresponding spectra are presented.

From Figure 6, note that values below 10^{-8} can be interpreted as zero eigenvalues. Then, in the case of S-DICCG$-$15 (Figure 6(b)), it can be observed that none of the $\mathcal{O}(10^{-6})-$eigenvalues of $M^{-1}A$ is eliminated after deflation, because they remain in the spectrum of $M^{-1}P_{W_\mathrm{S}}A$. Moreover, S-DICCG$-$63 converges very fast, since the $\mathcal{O}(10^{-6})-$eigenvalues vanish from the spectrum, as can be seen in Figure 6(d). Apparently, only for sufficiently large k, each deflation subdomain consists of a part of at most one bubble. Hence, the smallest eigenvalues can be eliminated, which confirms Conjecture 1.

With respect to the small $\mathcal{O}(1)-$eigenvalues, we observe in Figure 6(a) that they are approximately the same for ICCG and S-DICCG$-$15. Moreover, for the case of S-DICCG$-$63 (Figure 6(c)), it can be seen that the smallest $\mathcal{O}(1)-$eigenvalues do not appear in the spectrum of $M^{-1}P_{W_\mathrm{S}}A$. However, some other small eigenvalues around 0.1 can be noticed in Figure 6(c). Roughly speaking, the eliminated $\mathcal{O}(10^{-6})-$eigenvalues are moved to small eigenvalues of order 10^{-1}. Apparently, the eigenvectors associated with $\mathcal{O}(10^{-6})-$eigenvalues are not approximated accurately enough by the subdomain deflation vectors, even if we increase k. This may be caused by the fact that, by definition, the subdomain deflation vectors have the unfavorable property that they are disjunct (cf. Section 5.2). This can be remedied by using LS-DICCG$-k$ instead of S-DICCG$-k$, see Section 6.5.3.

6.5.2 Levelset Deflation

In Section 6.2, we have noticed that L-DICCG$-$4 reduces significantly the number of iterations, compared with ICCG. Figure 7 shows the 80 smallest eigenvalues of the corresponding spectra.

First it can be noticed in Figure 7(a), that $\mathcal{O}(1)-$eigenvalues are approximately the same for ICCG and L-DICCG$-$4. In Figure 7(b), we see that all $\mathcal{O}(10^{-6})-$eigenvalues are removed from $M^{-1}P_{W_\mathrm{L}}A$. However, they are moved to values in the vicinity of 0.2, see Figure 7(a). This is similar to the case of S-DICCG$-$63 (cf. Figure 6(c)). The only difference is that the smallest eigenvalues, associated with L-DICCG$-$4, are somewhat larger than those associated with S-DICCG$-$63.

As noticed in Sections 4.2 and 5.1, interfaces of bubbles should contribute to the deflation vectors. If one omits Lines 23–27 of Algorithm 1, where these interfaces are included in the levelset deflation vectors, then the convergence of L-DICCG$-$4 is significantly slower. In this case, it appears that $\mathcal{O}(10^{-6})-$eigenvalues are moved to eigenvalues between ϵ and 1.

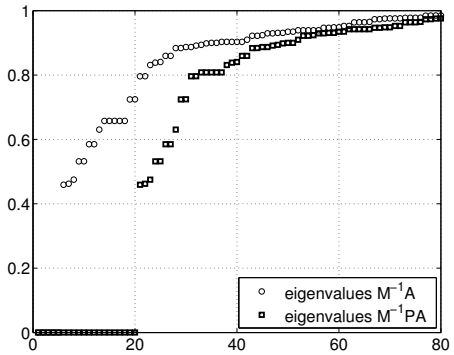

(a) Normal scale: S-DICCG−15.

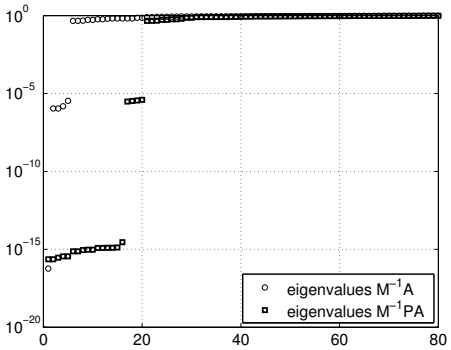

(b) Logarithmic scale: S-DICCG−15.

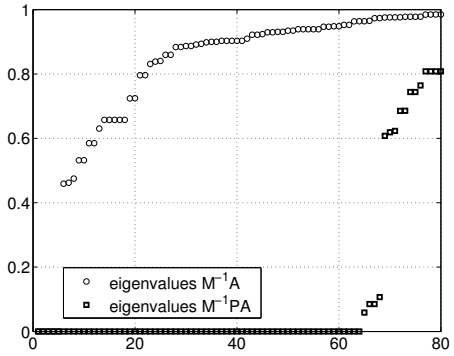

(c) Normal scale: S-DICCG−63.

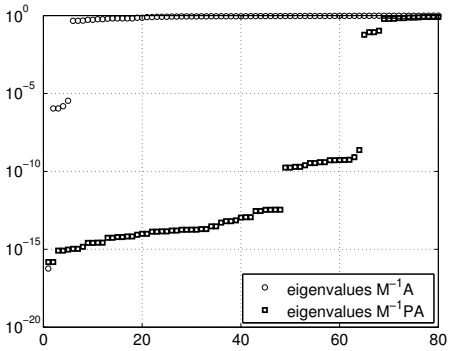

(d) Logarithmic scale: S-DICCG−63.

Figure 6: Eigenvalues of $M^{-1}A$ and $M^{-1}P_{W_S}A$ corresponding to S-DICCG−k, for the Poisson problem with $\epsilon = 10^{-6}$ and $n_x = n_y = 16$.

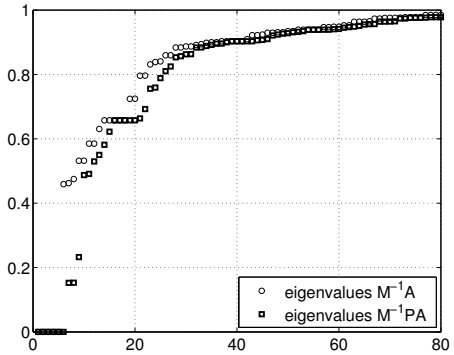

(a) Normal scale: L-DICCG−4.

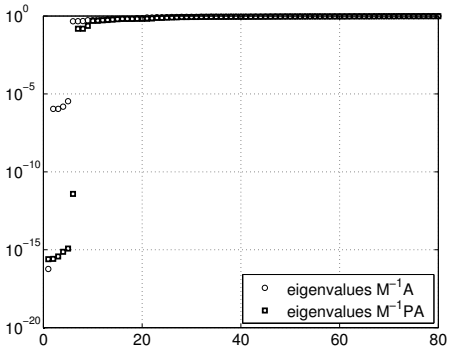

(b) Logarithmic scale: L-DICCG−4.

Figure 7: Eigenvalues of both $M^{-1}A$ and $M^{-1}P_{W_L}A$, corresponding to L-DICCG−5, for the Poisson problem with $\epsilon = 10^{-6}$ and $n_x = n_y = 16$.

6.5.3 Levelset Subdomain Deflation

As observed in Section 6.2, LS-DICCG$-k$ performs very well for all k. The related spectral plots can be found in Figure 8.

From Figure 8(a) and 8(b), we see that only $\mathcal{O}(10^{-6})-$eigenvalues disappear and all $\mathcal{O}(1)-$eigenvalues remain in the spectrum in the case of LS-DICCG-11. In Figure 8(c) and 8(d), it can be observed that both $\mathcal{O}(10^{-6})-$ and the smallest $\mathcal{O}(1)-$eigenvalues do not appear in the spectrum corresponding to LS-DICCG-35. More importantly, in contrast to the cases of S-DICCG$-k$ and L-DICCG$-k$, the elimination of $\mathcal{O}(10^{-6})-$eigenvalues by LS-DICCG$-k$ does not give rise to new eigenvalues between ϵ and 1. This is a favorable feature of levelset-subdomain deflation.

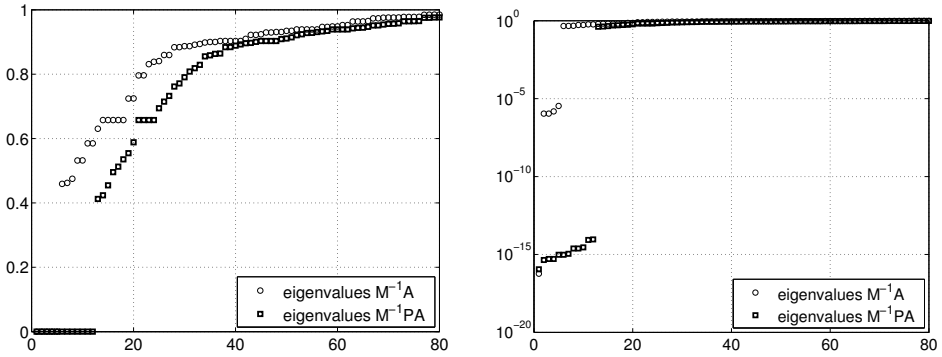

(a) Normal scale: LS-DICCG-11. (b) Logarithmic scale: LS-DICCG-11.

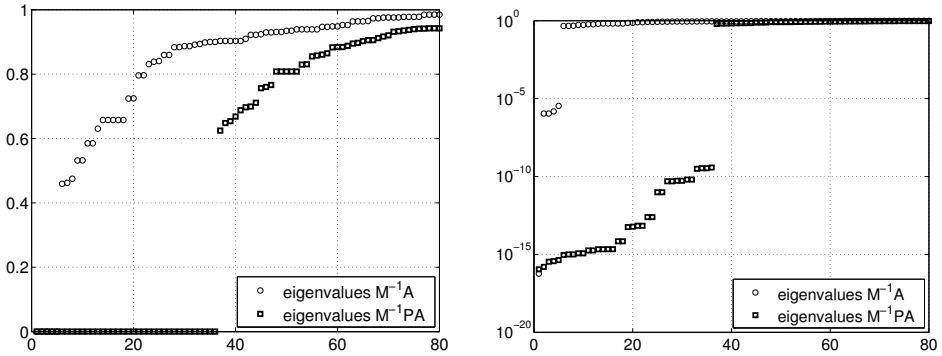

(c) Normal scale: LS-DICCG-35. (d) Logarithmic scale: LS-DICCG-35.

Figure 8: Eigenvalues of both $M^{-1}A$ and $M^{-1}P_{W_{\mathrm{LS}}}A$, corresponding to LS-DICCG$-k$, for the Poisson problem with $\epsilon = 10^{-6}$ and $n_x = n_y = 16$.

7 Conclusions

In [29, 30], it has been shown that DICCG with subdomain deflation vectors is efficient to solve linear systems coming from bubbly flow problems. In this paper, we have given more insight into explaining the efficiency of DICCG. This has been done by applying a spectral analysis to deflation with exact eigenvectors, and thereafter with perturbed eigenvectors. The main result is that eigenvectors, corresponding to the smallest eigenvalues, can be perturbed in such a way that they become sparse. In addition, based on this result, two new deflation variants have been

introduced and discussed. The first variant is the levelset deflation method, where the sparse deflation vectors are based on the geometry of the density field. The second variant, which is the levelset-subdomain deflation method, combines original subdomain deflation and levelset deflation, and has the advantages of both variants.

In the numerical experiments, we have compared the proposed deflation variants. It can be observed in most test cases that all of them perform very well compared with ICCG. It appears that subdomain deflation is only efficient for a sufficiently large number of subdomains. In this case, not only the smallest eigenvalues corresponding to the bubbles are eliminated, but also other small eigenvalues. Moreover, levelset deflation eliminates the smallest eigenvalues corresponding to bubbles at low cost, but leaves the other eigenvalues more or less untouched. For both of these methods, the elimination of the smallest eigenvalues may result in a spectrum that consists of eigenvalues which are obviously smaller than those of the cluster. It appears that levelset-subdomain deflation does not have this drawback. It is therefore an efficient method, although the work per iteration and the work to create the deflation vectors are significantly larger than for the other two variants. Moreover, all deflation variants (except for subdomain deflation with a small number of deflation vectors) are insensitive to large contrasts between the phases and the number of bubbles, and are efficient for all test cases with varying grid sizes.

It can be concluded that all deflation variants show good performance, and it depends on, among others, the geometry of problem and the maximum number of allowed deflation vectors, which of these variants is the most effective and efficient one.

Acknowledgments

We would like to thank the anonymous referees for their valuable remarks and comments, that enabled us to substantially improve this paper. Moreover, we also thank John Brusche for his contribution to Algorithm 1 and especially Pieter Wesseling for the helpful comments and thorough proof-reading of this manuscript.

References

[1] O. Axelsson and G. Lindskog, *On the Eigenvalue Distribution of a Class of Preconditioned Methods*, Numer. Math., **48**, 479–498 (1986).

[2] A.J. Cleary, R.D. Falgout, V.E. Henson, J.E. Jones, T.A. Manteuffel, S.F. McCormick, G.N. Miranda and J.W. Ruge, *Robustness and Scalability of Algebraic Multigrid*, SIAM J. Sci. Comput., **21**(5), 1064–8275 (2000).

[3] E. Cuthill and J. McKee, *Reducing the bandwidth of sparse symmetric matrices*, Proc. ACM Nat. Conf. Association of Computing Machinery, New York, 1969.

[4] J. E. Dendy, Jr., *Black Box Multigrid*, J. Comput. Phys., 48, 366–386 (1982).

[5] M. Dryja, *An additive Schwarz algorithm for two- and three dimensional finite element elliptic problems*, Domain Decomposition methods, SIAM Philadelphia, pp. 168–172, 1989.

[6] M. Dryja and O.B. Widlund, *Towards a unified theory of domain decomposition algorithms for elliptic problems*, Third International Symposium on Domain Decomposition Methods for Partial Differential Equations, SIAM Philadelphia, pp. 3–21, 1990.

[7] M. Dryja and O.B. Widlund, *Schwarz Methods of Neumann-Neumann Type for Three-Dimensional Elliptic Finite Element Problems*, Comm. Pure Appl. Math., **48**, 121–155 (1995).

[8] J. Frank and C. Vuik, *On the construction of deflation-based preconditioners*, SIAM J. Sci. Comp., **23**, 442–462 (2001).

[9] E.F. Kaasschieter, *Preconditioned conjugate gradients for solving singular systems*, J. Comp. Appl. Maths., **24**, 265–275 (1988).

[10] L.Y. Kolotilina, *Preconditioning of systems of linear algebraic equations by means of twofold deflation*, I. Theory, J. Math. Sci., **89**, 1652–1689 (1998).

[11] G.H. Golub and C.F. van Loan, *Matrix Computations*, Third Edition, The John Hopkins University Press, Baltimore, 1996.

[12] J. Mandel, *Balancing domain decomposition*, Commun. Appl. Numer. Meth., **9**, 233–241 (1993).

[13] J. Mandel, *Hybrid domain decomposition with unstructured subdomains*, Domain Decomposition Methods in Science and Engineering, Sixth International Conference of Domain Decomposition, Como, Italy, June 15–19, 1994.

[14] J. Mandel and M. Brezina, *Balancing domain decomposition for problems with large jumps in coefficients*, Math. Comp., **216**, 1387–1401 (1996).

[15] L. Mansfield, *Damped Jacobi preconditioning and coarse grid deflation for Conjugate Gradient iteration on parallel computers*, SIAM J. Sci. Stat. Comput., **12**, 1314–1323 (1991).

[16] J.A. Meijerink and H. A. Van der Vorst, *An iterative solution for linear systems of which the coefficient matrix is a symmetric M-matrix*, Math. Comp., **31**(137), 148–162 (1977).

[17] R.B. Morgan, *A restarted GMRES method augmented with eigenvectors*, SIAM J. Matrix Anal. Appl., **16**, 1154–1171 (1995).

[18] W. Mulder, S. Osher and J.A. Sethian, *Computing interface motion in compressible gas dynamics*. J. Comp. Phys., **100**, 209-228 (1992).

[19] R. Nabben and C. Vuik, *A comparison of Deflation and Coarse Grid Correction applied to porous media flow*, SIAM J. Numer. Anal., **42**, 1631–1647 (2004).

[20] R. Nabben and C. Vuik, *A Comparison of Deflation and the Balancing Preconditioner*, SIAM J. Sci. Comput., **27**, 1742–1759 (2006).

[21] R.A. Nicolaides, *Deflation of Conjugate Gradients with applications to boundary value problems*, SIAM J. Matrix Anal. Appl., **24**, 355–365 (1987).

[22] S. Osher, R.P. Fedkiw, *Level set methods: an overview and some recent results*, J. Comp. Phys., **169**, 463–502 (2001).

[23] S.P. van der Pijl, *Computation of bubbly flows with a mass-conserving level-set method*, PhD thesis, Delft University of Technology, 2005.

[24] S.P. van der Pijl, A. Segal, C. Vuik, and P. Wesseling, *A mass-conserving Level-Set method for modelling of multi-phase flows*, Int. J. Numer. Meth. Fluids , **47**, 339–361 (2005).

[25] Y. Saad, M. Yeung, J. Erhel and F. Guyomarc'h, *A deflated version of the Conjugate Gradient Algorithm*, SIAM J. Sci. Comput., **21**(5) 1909–1926 (2000).

[26] R. Scheichl and E. Vainikko, *Additive Schwarz and Aggregation-Based Coarsening for Elliptic Problems with Highly Variable Coefficients*, submitted (see also `http://www.bath.ac.uk/math-sci/BICS`), 2006.

[27] B. Smith, P. Bjørstad and W. Gropp, *Domain Decomposition*, Cambridge University Press, Cambridge, 1996.

[28] F.S. Sousa, N. Mangiavacchi, L.G. Nonato, A. Castelo, M.F. Tome, V.G. Ferreira, J.A. Cuminato and S. McKee, *A Front-Tracking / Front-Capturing Method for the Simulation of 3D Multi-Fluid Flows with Free Surfaces*, J. Comp. Physics, **198**, 469–499 (2004).

[29] J.M. Tang and C. Vuik, *On Deflation and Singular Symmetric Positive Semi-Definite Matrices*, **206**(2), 603-614 (2007).

[30] J.M. Tang and C. Vuik, *Efficient Deflation Methods applied to 3-D Bubbly Flow Problems*, Elec. Trans. Numer. Anal., **26**, 330–359 (2007).

[31] J.M. Tang and C. Vuik, *New Variants of Deflation Techniques for Bubbly Flow Problems*, Report 06-14, Delft University of Technology, ISSN 1389-6520, 2006.

[32] A. Toselli and O.B. Widlund. *Domain Decomposition: Algorithms and Theory*, Comp. Math., **34**, Springer, Berlin, 2005.

[33] C. Vuik, R. Nabben and J.M. Tang, *Deflation acceleration for Domain Decomposition Preconditioners*, Proc. 8th European Multigrid Conference on Multigrid, Multilevel and Multiscale Methods (Ed.: P. Wesseling, C.W. Oosterlee, P. Hemker), The Hague, The Netherlands, September 27-30, 2005.

[34] C. Vuik, A. Segal and J.A. Meijerink, *An efficient preconditioned CG method for the solution of a class of layered problems with extreme contrasts in the coefficients*, J. Comp. Phys., **152**, 385–403 (1999).

[35] C. Vuik, A. Segal, J.A. Meijerink and G.T. Wijma, *The construction of projection vectors for a Deflated ICCG method applied to problems with extreme contrasts in the coefficients*, J. Comp. Phys., **172**, 426–450 (2001).

[36] P. M. De Zeeuw, *Matrix-Dependent Prolongations and Restrictions in a Blackbox Multigrid Solver*, J. Comput. Appl. Math., **33**, 1–27 (1990).